

Published in final edited form as:

Acta Biomater. 2013 January ; 9(1): 4635–4644. doi:10.1016/j.actbio.2012.08.007.

Tuning 3D Collagen Matrix Stiffness Independently of Collagen Concentration Modulates Endothelial Cell Behavior

Brooke N. Mason^a, Alina Starchenko^a, Rebecca M. Williams^a, Lawrence J. Bonassar^{a,b}, and Cynthia A. Reinhart-King^{a,*}

^aDepartment of Biomedical Engineering, Cornell University, Ithaca, New York 14853, USA

^bDepartment of Mechanical and Aerospace Engineering, Cornell University, Ithaca, New York 14853, USA

Abstract

Numerous studies have described the effects of matrix stiffening on cell behavior using two dimensional (2D) synthetic surfaces; however less is known about the effects of matrix stiffening on cells embedded in three dimensional (3D) *in vivo*-like matrices. A primary limitation in investigating the effects of matrix stiffness in 3D is the lack of materials that can be tuned to control stiffness independently of matrix density. Here, we use collagen-based scaffolds where the mechanical properties are tuned using non-enzymatic glycation of the collagen in solution, prior to polymerization. Collagen solutions glycated prior to polymerization result in collagen gels with a 3-fold increase in compressive modulus without significant changes to the collagen architecture. Using these scaffolds, we show that endothelial cell spreading increases with matrix stiffness, as does the number and length of angiogenic sprouts and the overall spheroid outgrowth. Differences in sprout length are maintained even when the receptor for advanced glycation endproducts is inhibited. Our results demonstrate the ability to de-couple matrix stiffness from matrix density and structure in collagen gels, and that increased matrix stiffness results in increased sprouting and outgrowth.

Keywords

Extracellular Matrix; Angiogenesis; Collagen; Endothelial cell; Mechanical Properties; Stiffness

1. Introduction

The importance of the mechanical properties of the extracellular matrix (ECM) in mediating cell health and behavior is now well accepted. Changes in matrix stiffness have been shown to promote cardiovascular disease [1, 2] and cancer [3, 4] by altering cellular morphology [5], differentiation [6], traction force generation [7] focal adhesion formation [8] and cell migration dynamics [9]. Additionally, the mechanical properties of the ECM have been

© 2012 Acta Materialia Inc. Published by Elsevier Ltd. All rights reserved.

*Corresponding author: Cynthia A. Reinhart-King, 302 Weill Hall, 526 Campus Road, Ithaca, NY 14853, Tel: (607) 255-8491, Fax: (607) 255-7330, cak57@cornell.edu.

Conflict of Interest

The authors confirm that there are no known conflicts of interest associated with this publication and there has been no significant financial support for this work that could have influenced its outcome.

Publisher's Disclaimer: This is a PDF file of an unedited manuscript that has been accepted for publication. As a service to our customers we are providing this early version of the manuscript. The manuscript will undergo copyediting, typesetting, and review of the resulting proof before it is published in its final citable form. Please note that during the production process errors may be discovered which could affect the content, and all legal disclaimers that apply to the journal pertain.

found to be crucial regulators of the formation and arrangement of multi-cellular assemblies during tissue formation [10–13]. However, most studies investigating the role of matrix stiffening on cell behavior have primarily used 2D synthetic surfaces. As such, significantly less is known about the effects of matrix stiffening on cells embedded in three-dimensional (3D) *in vivo*-like matrices. This gap in knowledge is largely due to the lack of materials with tunable mechanical properties that are amenable to 3D cell culture.

Recent efforts to modulate 3D matrix stiffness have included modifying matrix density of natural proteins [14–17] and alginate [18], using synthetic polymers with tunable cross-linking densities such as poly(ethylene) glycol (PEG) to create hydrogel scaffolds [19, 20], and creating mixed matrices of natural proteins and other hydrogels such as agarose [16, 21, 22]. Although these modifications are capable of generating 3D scaffolds with tunable mechanical properties, they also change the fundamental structural properties of the culture system. For example, increasing the density of the matrix also causes changes in the porosity of the scaffold and the number of binding sites presented to the cells. Synthetic PEG-hydrogels offer the advantage of allowing for specific binding sequences to be incorporated at a specified density, independent of stiffness; however, PEG-hydrogels are amorphous and lack the native fiber structures found within most tissues. Alginate offers the ability to modulate stiffness in 3D, but it does not allow for cell migration because cells are unable to remodel it [18]. Therefore, while a number of approaches have been developed to modulate the stiffness of 3D culture, they each face limitations.

To develop and characterize 3D mechanically tunable scaffolds, we used non-enzymatic glycation to stiffen naturally-derived collagen [23, 24]. Non-enzymatic glycation is a process whereby proteins are crosslinked by reducing sugars such as glucose or ribose through a sequence of chemical modifications known as the Maillard reaction [25, 26]. During non-enzymatic glycation, reducing sugars interact with amino groups on proteins to form Schiff bases that can rearrange into Amadori products [27]. These Amadori products subsequently form advanced glycation endproducts (AGE) that accumulate on proteins and cause cross-link formation. A number of studies have utilized non-enzymatic glycation to create stiffer collagen scaffolds with increased mechanical integrity by incubating polymerized collagen gels with reducing sugar solutions [28, 29]. However, since an excess of sugars create a hyperosmotic extracellular environment, this technique has been limited to stiffening scaffolds prior to seeding cells onto the surface of the gels and does not allow cells to be embedded within the ECM scaffold prior to gel polymerization. Notably, others have used collagen gels glycated with glucose-6-phosphate post-polymerization to investigate endothelial cell response [30]. However, the limitations of this system include the inability to examine sparse cellular cultures and unclear effects to the collagen architecture as a result of cell injection. By glycating the collagen prior to polymerization, we are able to observe immediate spreading and migration effects of single cells or multi-cellular aggregates without disruption of the collagen architecture.

In addition to the role of AGEs in modulating the mechanical properties of the extracellular environment, some cells possess receptors for advanced glycation endproducts (RAGE) that can influence intracellular signaling [31, 32]. Interestingly, the engagement of these receptors on cells is thought to be a factor in a number of disease states including diabetes, atherosclerosis, Alzheimer's, cataracts, and cancer [33–37] and RAGE signaling has been shown to affect endothelial cell responses [38].

Here, we glycate the collagen prior to polymerization, which allows for cell encapsulation at the time of gelation [23, 24]. Using this technique, cells can be embedded within collagen gels and the collagen density can be kept constant while mechanical stiffness is varied. We characterized the fiber structure of glycated collagen gels and show that there exists a

regime where stiffness can be increased 3-fold with only minimal changes in fiber architecture and no change in collagen density.

To investigate the effects of changes in 3D matrix stiffness on cell behavior, we embedded individual bovine aortic endothelial cells (ECs) or cellular spheroids in collagen of varying stiffness. Our data indicate that both individual cell spreading and the growth of angiogenic sprouts increase with matrix stiffness. We also found that even when the AGE/RAGE interaction is inhibited, spheroid outgrowth increases with the stiffness of the matrix. Together, our study describes a tractable method for modulating 3D matrix stiffness independently of collagen structure, and using these materials, we demonstrate that matrix stiffness in 3D plays a critical role in modulating endothelial cell behavior.

2. Materials and Methods

2.1 Cell Culture

2.1.1 EC Culture—Bovine aortic endothelial cells (ECs) were purchased from VEC Technologies (Rensselaer, NY) and used until passage 12 as described previously [11]. Briefly, cells were fed every other day and grown to confluence at 37°C and 5% CO₂ in Medium 199 (Invitrogen, Carlsbad, CA) supplemented with 10% Fetal Clone III (HyClone, Logan, UT) and 1% each of MEM Amino Acids (Invitrogen), MEM Vitamins (Mediatech, Manassas, VA), and penicillin-streptomycin (Invitrogen).

2.1.2 Spheroid Generation—ECs were suspended in complete Medium 199 supplemented with 0.25% Methocult (StemCell Technologies, Vancouver, BC, Canada) and seeded at 10,000 cells/well in non-adherent 96-well round bottom plates (Costar, Corning Incorporated, Corning, NY). Plates were centrifuged to pellet the cells and placed on an orbital shaker at 37°C and 5% CO₂ for 2 hours to facilitate spheroid formation. EC spheroids were cultured for 2 days in the plates prior to embedding within collagen gels to allow for spheroid compaction.

2.2 Preparation of Collagen Gels

2.2.1 Isolation and Non-enzymatic Glycation of Collagen—Type I collagen was isolated from rat tail tendons (Pel-Freez Biologicals, Rogers, AR) and extracted in 0.1% sterile acetic acid (JT Baker, Phillipsburg, NJ) at 4°C. The resulting solution was centrifuged to remove solids and the supernatant was lyophilized and then solubilized in 0.1% sterile acetic acid to form 10 mg/mL stock solutions. As described previously, collagen stock solutions were mixed with 0.5 M ribose to form glycated collagen solutions containing a final concentration of 0, 50, 100, 150, 200, or 250 mM ribose in 0.1% sterile acetic acid and incubated at 4°C for 5 days [23, 24]. Glycated collagen solutions were neutralized with 1 M sodium hydroxide in 10X D-PBS buffer and mixed with HEPES (EMD Millipore, Billerica, MA) and sodium bicarbonate (JT Baker) in 10X D-PBS (Invitrogen) to form 1.5 mg/mL collagen gels with final concentrations of 1X D-PBS, 25 mM HEPES, and 44 mM sodium bicarbonate.

2.2.2 Fluorescent Labeling of Collagen—Collagen was labeled with tetramethylrhodamine isothiocyanate (TRITC) (Invitrogen) as has been described previously [39, 40]. Briefly, lyophilized collagen was mixed with 0.1 M, pH 9 sodium bicarbonate (JT Baker) to achieve a final collagen concentration of 10 mg/ml. TRITC in DMSO was then added at a 1:30 dilution to the collagen and allowed to react in the dark for 24 hours at 4°C. The labeled collagen solution was then dialyzed extensively against 0.1% sterile acetic acid using dialysis tubing with a 20,000 MW cutoff (Spectrum Laboratories, Inc, Rancho Dominguez, CA).

2.2.3 Cell and Spheroid Embedding—Isolated cells or spheroids were mixed with neutralized collagen solutions. Collagen gels were allowed to polymerize at 37°C and then overlaid with complete medium. Medium was changed at 1 hour and then every other day during experiments. When investigating the effects of the receptors for advanced glycation endproducts (RAGE) on spheroid outgrowth, a polyclonal anti-RAGE antibody (N-16, Santa Cruz Biotechnology, Inc, Santa Cruz, CA) was added to spheroids to inhibit the interaction of RAGE with AGE. The anti-RAGE antibody was added at 10 µg/ml in complete medium to embedded spheroids after the spheroids had been incubated for a 1 hour with complete medium. Spheroids treated with the anti-RAGE antibody were monitored over the course of 2 days for extension outgrowth [41–45]. In cases where isolated cells were not suspended within the gel, an equivalent volume of complete medium was added to the gel to maintain gel composition between experiments.

2.3 Collagen Polymerization Assay

The polymerization of collagen gels at 37°C was monitored by measuring the absorbance of the collagen solutions every 3 minutes at 500 nm using a Synergy HT microplate reader (BioTek, Winooski, VT). Polymerization curves were fit with a variable slope sigmoidal dose-response curve and the slope of linear portion of the curve was reported as the fibril formation rate (GraphPad Prism, GraphPad Software, Inc, La Jolla, CA).

2.4 Mechanical Testing of Collagen Gels

The equilibrium compressive modulus of collagen gels was quantified as described previously [24]. Briefly, an Enduratec EL2100 frame (Bose, Eden Prairie, MN) with a 250-g load cell was used to measure the resultant forces of 75 micron displacements on 6 mm × 1.5 mm collagen gels in a confined compression chamber. A standard linear solid model of viscoelastic behavior was used to fit the stress relaxation data by using the equation, $\sigma_{eq} = A(1 - e^{-t/\tau}) + B$, where B is the instantaneous stress and $A + B$ is the equilibrium stress, t is time, and τ is the exponential time constant [24, 39]. The equilibrium modulus was calculated as the slope of the linear region of the stress-strain curve. Similarly to other studies of collagen gel mechanical properties, we assumed that the collagen gels were isotropic and elastic [39, 46].

2.5 Cellular Proliferation Assay

ECs were suspended at 250,000 cells/ml of collagen and cultured for up to 3 weeks. Collagen gels were collected at 0, 1, 2, 3 weeks and frozen at -20°C. The gels were digested for 14 hours at 60°C with papain and the DNA content of the gels was quantified with a Quant-iT PicoGreen dsDNA Kit (Invitrogen) using a Synergy HT microplate reader (BioTek). Total DNA content per gel were normalized to DNA content at day 0 for each experiment and then experiments were averaged (N=3).

2.6 Imaging

2.6.1 Confocal Reflectance Collagen Imaging—The internal structure of collagen gels was visualized with confocal reflectance microscopy using a Zeiss LSM700 inverted laser scanning confocal microscope (Carl Zeiss, Oberkochen, Germany). Samples were illuminated with a 405 nm laser and optical slices 1 micron in depth were collected with a long working distance water-immersion C-Apochromat 40×/1.1 NA objective (Carl Zeiss) [47]. Image acquisition parameters were kept the same for all gels.

2.6.2 Image Autocorrelation Analysis—To compare the structural properties of the collagen gels, an autocorrelation analysis was performed on the confocal reflectance microscopy images [48, 49]. Briefly, each image was translated with respect to itself in all

directions (2D) and the average length of intensity correlation between the images was measured. The decay in the correlation between the images was used to determine the mean characteristic length of features (collagen fibers) within the image. The mean characteristic lengths were plotted for each image and coincide with the mean fibril length, the average fibril distribution and the extent of bundling within the collagen gel.

2.6.3 Single Cell and Spheroid Imaging and Analysis—Isolated cells were imaged on a Zeiss CSU-X1 (Carl Zeiss) spinning disc confocal and each z-stack was projected onto a single plane using the ImageJ maximum intensity feature (ImageJ 1.44p, NIH). The resulting 2D cellular images were used to quantify projected cell areas and perimeters ($n = 138$ – 148) [50–52]. Multi-cellular spheroids were imaged with brightfield on a Zeiss Axio Observer Z1m (Carl Zeiss) and with fluorescence on a Zeiss LSM700 point scanning confocal. Brightfield images of spheroids after 1 day in culture were compared to images of the spheroids at the time of embedding and analyzed for the number and length of extensions emanating from the spheroids ($n = 18$ – 23). Additionally, brightfield images were used to quantify the area of both control spheroids ($n = 17$ – 18) and spheroids treated with anti-RAGE antibody ($n=16$ – 23) over time. Control data sets of spheroid outgrowth were collected independently.

2.6.4 Staining—Cells within collagen gels were fixed with 3.7% (v/v) formaldehyde in PBS, permeabilized with 1% (v/v) Triton (JT Baker) in PBS, and stained for actin with Alexa Fluor 488 phalloidin (Invitrogen) in PBS/1% (w/v) bovine serum albumin (BSA, Sigma-Aldrich, St. Louis, MO) and for DNA with DAPI (Sigma-Aldrich) in purified deionized water.

2.7 Statistics

Data were analyzed using a one-way analysis of variance (ANOVA) and Tukey's Honest Significant Difference test in JMP (SAS, v.8.0 and v.9.0) with statistical significance considered as $p < 0.05$. All values are expressed as the mean \pm SEM.

3. Results

3.1 Non-enzymatic Glycation Affects Collagen Gel Mechanical and Structural Properties

The mechanical properties of collagen gels were modulated by incubating unpolymerized collagen solutions with 0 – 250 mM ribose for 5 days prior to collagen neutralization and polymerization. The equilibrium compressive modulus was measured by applying a 5% stepwise strain to a confined collagen gel, measuring the resultant force, and fitting the data to a standard linear solid model of viscoelastic behavior. Collagen gels polymerized after non-enzymatic glycation have an increased equilibrium compressive modulus that varies approximately linearly with ribose concentration (Fig. 1). Over the range of ribose concentrations tested, the compressive modulus of the collagen gels increased approximately 4-fold (from ~ 175 Pa to ~ 730 Pa).

To investigate the effects of non-enzymatic glycation on collagen gel fiber architecture, the gels were imaged with confocal reflectance and fluorescence microscopy. Collagen solutions glycosylated with 0 – 100 mM ribose form gels that have qualitatively similar fiber distributions and arrangements; whereas collagen solutions treated with 150 – 250 mM ribose form gels with larger, more prominent collagen fibers when imaged either confocal reflectance (Fig. 2a) or fluorescence microscopy (Fig. 3). To further characterize the fiber architecture of the glycosylated collagen gels, an image autocorrelation analysis was performed. The autocorrelation mean radius is a measure of the size over which fibril structures persist in the image. The autocorrelation data indicated that collagen gels treated with 0 – 100 mM

ribose have similar fibril sizes and arrangements, while higher ribose concentrations generate populations of larger fibrils in confocal reflectance images (Fig. 2b).

Because differences in fiber structure have been shown previously to be correlated with differences in polymerization dynamics [53, 54], the effects of non-enzymatic glycation on collagen gel polymerization dynamics were investigated with an absorbance assay. During polymerization, collagen fibril formation causes an increase in opacity that can be directly measured by absorbance. Collagen polymerization dynamics can generally be described by three stages and correspond to a sigmoidal curve that are observed with the absorbance assay: the nucleation phase is denoted by the toe region of the curve, the fibril formation phase is denoted by the linearly increasing portion of the curve, and the fibril stabilization phase is denoted by the plateau region of the curve. Non-enzymatic glycation increased the nucleation time of collagen fibril formation (Fig. 4a). Notably, the rate of fibril formation showed a comparable trend to the autocorrelation data and was very similar for collagen incubated with 0 – 100 mM ribose and was significantly altered for collagen solutions that had been treated with 150 – 250 mM ribose (Fig. 4b). These results indicate that the extent of glycation can alter the polymerization dynamics of collagen gels.

3.2 Endothelial Cell Viability and Proliferation in Glycated Collagen Gels

To evaluate the effect of collagen glycation on cell proliferation, ECs were embedded within collagen gels, and DNA content was quantified at 0, 7, 14, and 21 days. ECs remained viable and proliferated at similar levels within glycated collagen gels and controls during the 3 week proliferation assay (Fig. 5). These results indicate that collagen glycation prior to gel polymerization does not alter EC proliferative potential and that the cells remain viable within the gel.

3.3 Changes in 3D Matrix Stiffness Increase Cell Spreading

Studies using 2D planar substrates have reported that increased matrix stiffness results in increased cell spreading [55]. To assess whether modulating collagen stiffness independently of collagen organization caused cellular morphological changes in 3D matrices, ECs were embedded within collagen gels that had been glycated with 0 – 100 mM ribose and imaged with confocal microscopy. Ribose concentrations ranging from 0 – 100 mM were chosen because our data indicate that the structure of the collagen is only minimally altered (Fig. 2 and Fig. 3) while the compressive modulus increases from ~175 to ~515 Pa (Fig. 1). ECs appeared well-spread with an elongated morphology and displayed defined actin fibrils in each stiffness condition studied (Fig. 6a). Interestingly, EC projected area and perimeter were both significantly increased as a function of matrix stiffness (Fig. 6b–c), indicating that stiffness is a mediator of cell spreading in 3D matrices.

3.4 Increased Matrix Stiffness Enhances Spheroid Outgrowth

Our lab has previously shown that endothelial cell network formation can be modulated by both matrix stiffness and ligand density in 2D [11]. To investigate whether endothelial sprouting is altered by collagen stiffness in 3D, EC spheroids were embedded within glycated collagen and the formation of sprouts from the spheroids was monitored over several days. Notably, increasing the stiffness of the collagen visibly altered the morphology of the outgrowths emanating from the spheroids (Fig. 7a). While spheroids in all gels displayed a robust sprouting response, those cultured within the softer gels had fewer extensions that appeared to be less branched than the spheroids cultured within the stiffer, glycated gels. After only one day, spheroids within the stiffest collagen gels (100 mM ribose), had a 2-fold increase in the total extension length per spheroid and a 1.5-fold increase in the average number of extensions per spheroids when compared to spheroids cultured within the soft collagen gels (0 mM ribose) (Fig. 7b–c). Additionally, spheroids in

the stiffest collagen gels (100 mM ribose) had a significantly larger projected area during the entire 5 day analysis period than those in soft gels (0 mM ribose) (Fig. 7d). These data indicate that 3D matrix stiffness altered endothelial sprouting dynamics. To determine if the differences in extension morphology persisted in long-term spheroid culture, EC spheroids were embedded and grown for 8 days. The resulting sprouts were stained for actin and DAPI and imaged using confocal microscopy (Fig. 8). The morphology of spheroid outgrowth remained altered dependent upon collagen stiffness. To investigate the effects of AGE/RAGE signaling relative to stiffness on spheroid outgrowth, RAGE were inhibited with an anti-RAGE blocking antibody [41]. Notably, although the overall spheroid outgrowth was decreased with anti-RAGE treatment when compared to controls, the EC spheroid outgrowth remained significantly increased in the stiffer collagen gels at day 2 (Fig. 9).

4. Discussion

While numerous studies have investigated the role of matrix stiffness in mediating cell behavior on 2D substrates, much less is known about cell response to matrix stiffness in 3D matrices. Here, we describe and characterize a method to modulate the 3D stiffness of native, fibrillar collagen matrices while only minimally altering the inherent fiber structure, without the addition of synthetic materials. Using non-enzymatic glycation, collagen gel stiffness can be increased 3-fold while only minimally changing the fiber architecture. Further, the method described permits isolated cells or multi-cellular spheroids to be embedded within the glycated collagen gels during polymerization so that the resulting cellular response to 3D stiffness can be studied. Our data indicate that increasing the collagen gel modulus from ~175 Pa to ~515 Pa causes changes in cell spreading and dramatic differences in the morphology of endothelial sprouts from spheroids. These results demonstrate the utility non-enzymatic glycation to alter 3D matrix mechanics with minimal changes in collagen fibril organization so that cell response to 3D changes in matrix stiffness can be studied.

Methods to glycate collagen have been explored previously in the literature. Several reports have described methods to glycate collagen gels once they have been polymerized [28, 29] or to adsorb glycated collagen to glass or plastic [56]. However, neither of these methods allow for cells to be embedded within the collagen. Other studies have reported glycating collagen gels prior to polymerization [23, 24, 57], however it was not clear what effect the process of glycation was having on the fiber architecture. Because fiber architecture is known to alter cell behavior [58], it is important to develop scaffolds where it is possible to control stiffness without altering fiber diameter or distribution. Here, we identify a range of ribose concentrations where stiffness can be increased with minimal changes to fiber architecture. Our data show that collagen glycated with 0 – 100 mM ribose exhibits a compressive modulus that varies over three fold (~175 Pa to ~515 Pa) (Fig. 1) without significant changes to the fibril formation rates or fiber arrangements. At higher concentrations of ribose (150 – 250 mM), the compressive modulus of the gels increases, but a change in the fibril length (Fig. 2 and Fig. 3) and a decrease in the rate of gel polymerization (Fig. 4) also occur. Therefore, while glycation can tune the modulus of collagen by 4-fold, the changes in modulus that can be controlled while not producing statistically significant changes in fiber architecture fall within a narrower range. It is important to note the ligand availability and pore size can also affect cell behavior, although we did not directly test for these parameters here.

Notably, the changes in fiber architecture due to glycation (Fig. 2 and Fig. 3) coincide with changes in the polymerization dynamics (Fig. 4) of collagen treated with varying concentrations of ribose. Polymerization rate has been shown to be affected by a number of other parameters as well, including pH [59], temperature [60, 61], and the presence of ions

[62], where pore structure and fiber length and diameter are also altered. These results suggest that the polymerization rate of the collagen gels may be responsible for the changes in the fiber architecture we observe for collagen incubated with high concentrations of ribose. Further modulation of the polymerization kinetics using temperature or pH may allow for the formation of highly glycosylated collagen gels that resemble the architecture of gels glycosylated with 0 – 100 mM ribose.

While stiffness has been shown to modulate numerous cellular behaviors, these reports are largely based on studies using 2D substrates. It is not clear how results based on the use of 2D substrates translate into behaviors in 3D. In previous work, we showed that changes in substrate stiffness resulted in changes in cell spreading [55]. Our data using 3D glycosylated gels indicate that, similar to our results obtained in 2D cultures, endothelial cells increase their spreading due to increased matrix stiffness. Unlike many studies using 2D substrates, we find no change in endothelial cell proliferation rates in 3D due to stiffness (Fig. 5). These results may be attributed to the complex relationship of cell division with spreading and matrix deposition, degradation, and remodeling in 3D matrices [63, 64]. However, just as cell response to matrix stiffness on 2D substrates has been found to be cell-type specific [65], it is likely that cell response in 3D matrices is also cell-type specific and should be further investigated.

In our study, we observed a significant increase in cellular spreading and extension formation with increasing matrix stiffness almost immediately (within 24 hours) after the individual cells and multi-cellular spheroids were embedded (Fig. 6 and Fig. 7) and these effects persisted throughout the entire course of our culture (8 days) (Fig. 8). Interestingly, work by Francis-Sedlak et al. reported a transient and opposite response to matrix stiffness when human umbilical vein endothelial cell aggregates were injected into gels glycosylated with glucose-6-phosphate post-polymerization [30]. A number of differences in experimental design could attribute for these discrepancies including the density of the collagen matrices, cell type, or methods of glycosylation and cellular embedding. Additionally, collagen glycosylation has been shown to decrease adherent cell adhesion and mechanotransduction by modifying integrin binding sites [56, 66–68]. Interestingly, we found that spheroids and isolated cells within the stiffer, glycosylated matrices have increased extension outgrowth and spreading when compared to those in non-glycosylated matrices (Figs. 6–8). While we did not directly investigate cell adhesion in our study, our findings suggest that, if glycosylation in our system does decrease ligand availability, endothelial cells within glycosylated matrices integrate mechanical cues and increase their spreading even if cell adhesion is disrupted when compared to the non-glycosylated matrices. Others have also shown that increasing the amount of non-enzymatic glycosylation cross-linking decreases the degradability of matrices [30, 69, 70]. It is notable that we saw the most spheroid outgrowth in the stiffest, least degradable, and least adhesive collagen matrices (Fig. 7). Future studies should elucidate whether our results are universal responses for all endothelial cell sources or specific to bovine aortic endothelial cells and further experiments should be performed to determine the relative effects of matrix density, glycosylation, and matrix degradation on cell outgrowth and function in collagen matrices.

In vivo, the cross-linking of matrix proteins via non-enzymatic glycosylation is a slow process that occurs naturally, resulting in AGE cross-links that cause tissue stiffening with age. Cross-link accumulation is accelerated in diseases where blood sugar levels are not well-regulated such as diabetes [69–71]. Glycosylation has the most profound effect on components within the body that have a low turnover rate, including collagen [70]. Tissues including the vasculature [72], bone [73], cornea [74], and skin [75] and diseases such as Alzheimer's [76], rheumatoid arthritis [77], and end stage renal disease [78] have all been associated with the formation of glycosylation cross-links. In this study we have shown that collagen gel

stiffness alters spheroid outgrowth when the AGE/RAGE interaction is inhibited (Fig. 9). Notably, spheroid outgrowth decreased in RAGE inhibited spheroids when compared to control spheroids in matrices of the same stiffness, suggesting that the presence of the AGE/RAGE interaction may play a role in promoting extension formation and outgrowth. The concentrations and experimental time points we chose were similar to other studies using anti-RAGE antibodies for blocking [41–45], however it is not clear if the antibody completely blocks the interaction between AGE/RAGE at the concentrations used. To determine the relative roles of chemical versus mechanical changes due to glycation, additional experiments are required and are an interesting area of future work given the effects of glycation on many major tissues in the body. Better models using collagen glycation may not only enable a greater understanding of how matrix stiffness affects cells in 3D but also how glycation can promote disease.

In both solid tumor growth and diabetes, tissues tend to stiffen [72, 79] and, in both disease states, angiogenesis is perturbed and vessels tend to be malformed and present abnormally [80, 81]. Our results suggest that the stiffening of the matrix may be one mechanism which causes changes in the quantity and organization of blood vessels. In our study, differences in the number of extensions per spheroids were measurable as early as one day after embedding (Fig. 7) indicating that the cells were integrating the stiffness cues into their behavior in the early stages of extension formation. Notably, the morphological differences in the extensions with stiffness were maintained throughout the entire length of culture indicating that matrix stiffness likely plays a key role in angiogenesis.

5. Conclusions

The study describes a tractable technique for modifying collagen stiffness independently of gel density and fiber structure. By glycating the collagen while in solution, we were able to embed cells within collagen matrices to examine the effects of 3D stiffness on individual- and multicellular behaviors. These changes in stiffness significantly altered endothelial cell morphology and 3D sprouting from spheroids, indicating that the 3D mechanical environment is an essential mediator of cellular response. In the future, non-enzymatic glycation could be used to study the effects of extracellular matrix stiffness on a range of cell types that have previously been shown to be influenced by changes in matrix stiffness in 2D systems such as neurons [4], stem cells[6], and vascular smooth muscle cells [2].

Acknowledgments

This work was supported by the Cornell Center on the Microenvironment & Metastasis through Award Number U54CA143876 from the National Cancer Institute, by the National Center for Research Resources and the National Institute of General Medicine of the National Institutes of Health through Grant Number R21RR025801, and the National Science Foundation Graduate Research Fellowship Program (BNM). We gratefully acknowledge the work of Yun-shao Sung, Rafael Gonzalez-Cruz, and Shaoyang Yeh for their helpful input and discussions.

References

1. Huynh J, Nishimura N, Rana K, Peloquin JM, Califano JP, Montague CR, et al. Age-related intimal stiffening enhances endothelial permeability and leukocyte transmigration. *Sci Transl Med*. 2011; 3:112ra22.
2. Isenberg BC, Dimilla PA, Walker M, Kim S, Wong JY. Vascular smooth muscle cell durotaxis depends on substrate stiffness gradient strength. *Biophys J*. 2009; 97:1313–22. [PubMed: 19720019]
3. Paszek MJ, Zahir N, Johnson KR, Lakins JN, Rozenberg GI, Gefen A, et al. Tensional homeostasis and the malignant phenotype. *Cancer Cell*. 2005; 8:241–54. [PubMed: 16169468]

4. Ulrich TA, de Juan Pardo EM, Kumar S. The mechanical rigidity of the extracellular matrix regulates the structure, motility, and proliferation of glioma cells. *Cancer Res.* 2009; 69:4167–74. [PubMed: 19435897]
5. Yeung T, Georges PC, Flanagan LA, Marg B, Ortiz M, Funaki M, et al. Effects of substrate stiffness on cell morphology, cytoskeletal structure, and adhesion. *Cell Motility and the Cytoskeleton.* 2005; 60:24–34. [PubMed: 15573414]
6. Engler AJ, Sen S, Sweeney HL, Discher DE. Matrix elasticity directs stem cell lineage specification. *Cell.* 2006; 126:677–89. [PubMed: 16923388]
7. Reinhart-King CA, Dembo M, Hammer DA. Endothelial cell traction forces on RGD-derivatized polyacrylamide substrata. *Langmuir.* 2003; 19:1573–9.
8. Beningo KA, Dembo M, Kaverina I, Small JV, Wang YL. Nascent focal adhesions are responsible for the generation of strong propulsive forces in migrating fibroblasts. *J Cell Biol.* 2001; 153:881–8. [PubMed: 11352946]
9. Pelham RJ Jr, Wang Y. Cell locomotion and focal adhesions are regulated by substrate flexibility. *Proc Natl Acad Sci U S A.* 1997; 94:13661–5. [PubMed: 9391082]
10. Guo WH, Frey MT, Burnham NA, Wang YL. Substrate rigidity regulates the formation and maintenance of tissues. *Biophysical Journal.* 2006; 90:2213–20. [PubMed: 16387786]
11. Califano JP, Reinhart-King CA. A Balance of Substrate Mechanics and Matrix Chemistry Regulates Endothelial Cell Network Assembly. *Cellular and Molecular Bioengineering.* 2008; 1:122–32.
12. Reinhart-King CA, Dembo M, Hammer DA. Cell-Cell Mechanical Communication through Compliant Substrates. *Biophysical Journal.* 2008; 95:6044–51. [PubMed: 18775964]
13. Shebanova O, Hammer DA. Biochemical and Mechanical Extracellular Matrix Properties Dictate Mammary Epithelial Cell Assembly. *Biotechnol J.* 2011
14. Kniazeva E, Putnam AJ. Endothelial cell traction and ECM density influence both capillary morphogenesis and maintenance in 3-D. *Am J Physiol Cell Physiol.* 2009; 297:C179–87. [PubMed: 19439531]
15. Shamloo A, Heilshorn SC. Matrix density mediates polarization and lumen formation of endothelial sprouts in VEGF gradients. *Lab Chip.* 2010; 10:3061–8. [PubMed: 20820484]
16. Rao RR, Peterson AW, Ceccarelli J, Putnam AJ, Stegemann JP. Matrix composition regulates three-dimensional network formation by endothelial cells and mesenchymal stem cells in collagen/fibrin materials. *Angiogenesis.* 2012; 15:253–64. [PubMed: 22382584]
17. Sieminski AL, Heibel RP, Gooch KJ. The relative magnitudes of endothelial force generation and matrix stiffness modulate capillary morphogenesis in vitro. *Exp Cell Res.* 2004; 297:574–84. [PubMed: 15212957]
18. Genes NG, Rowley JA, Mooney DJ, Bonassar LJ. Effect of substrate mechanics on chondrocyte adhesion to modified alginate surfaces. *Arch Biochem Biophys.* 2004; 422:161–7. [PubMed: 14759603]
19. Kraehenbuehl TP, Zammaretti P, Van der Vlies AJ, Schoenmakers RG, Lutolf MP, Jaconi ME, et al. Three-dimensional extracellular matrix-directed cardioprogenitor differentiation: systematic modulation of a synthetic cell-responsive PEG-hydrogel. *Biomaterials.* 2008; 29:2757–66. [PubMed: 18396331]
20. Straley KS, Heilshorn SC. Independent tuning of multiple biomaterial properties using protein engineering. *Soft Matter.* 2009;5.
21. Ulrich TA, Jain A, Tanner K, MacKay JL, Kumar S. Probing cellular mechanobiology in three-dimensional culture with collagen-agarose matrices. *Biomaterials.* 2010; 31:1875–84. [PubMed: 19926126]
22. Ulrich TA, Lee TG, Shon HK, Moon DW, Kumar S. Microscale mechanisms of agarose-induced disruption of collagen remodeling. *Biomaterials.* 2011; 32:5633–42. [PubMed: 21575987]
23. Roy R, Boskey AL, Bonassar LJ. Non-enzymatic glycation of chondrocyte-seeded collagen gels for cartilage tissue engineering. *Journal of Orthopaedic Research.* 2008; 26:1434–9. [PubMed: 18473383]
24. Roy R, Boskey A, Bonassar LJ. Processing of type I collagen gels using nonenzymatic glycation. *Journal of Biomedical Materials Research Part A.* 2010; 93A:843–51. [PubMed: 19658163]

25. Ulrich P, Cerami A. Protein glycation, diabetes, and aging. *Recent Prog Horm Res.* 2001; 56:1–21. [PubMed: 11237208]
26. Maillard L. Action des acides amines sur les sucres: formation des melanoïdes par voie méthodique. *Comptes Rendus de l'Académie des Sciences.* 1912; 154:66–8.
27. Hodge JE. The Amadori rearrangement. *Adv Carbohydr Chem.* 1955; 10:169–205. [PubMed: 13292324]
28. Girton TS, Oegema TR, Tranquillo RT. Exploiting glycation to stiffen and strengthen tissue equivalents for tissue engineering. *J Biomed Mater Res.* 1999; 46:87–92. [PubMed: 10357139]
29. Francis-Sedlak ME, Uriel S, Larson JC, Greisler HP, Venerus DC, Brey EM. Characterization of type I collagen gels modified by glycation. *Biomaterials.* 2009; 30:1851–6. [PubMed: 19111897]
30. Francis-Sedlak ME, Moya ML, Huang J-J, Lucas SA, Chandrasekharan N, Larson JC, et al. Collagen glycation alters neovascularization in vitro and in vivo. *Microvascular Research.* 2010; 80:3–9. [PubMed: 20053366]
31. Basta G, Lazzzerini G, Massaro M, Simoncini T, Tanganelli P, Fu C, et al. Advanced glycation end products activate endothelium through signal-transduction receptor RAGE: a mechanism for amplification of inflammatory responses. *Circulation.* 2002; 105:816–22. [PubMed: 11854121]
32. Brett J, Schmidt AM, Yan SD, Zou YS, Weidman E, Pinsky D, et al. Survey of the distribution of a newly characterized receptor for advanced glycation end products in tissues. *Am J Pathol.* 1993; 143:1699–712. [PubMed: 8256857]
33. Thomas MC, Baynes JW, Thorpe SR, Cooper ME. The role of AGEs and AGE inhibitors in diabetic cardiovascular disease. *Curr Drug Targets.* 2005; 6:453–74. [PubMed: 16026265]
34. Reddy VP, Obrenovich ME, Atwood CS, Perry G, Smith MA. Involvement of Maillard reactions in Alzheimer disease. *Neurotox Res.* 2002; 4:191–209. [PubMed: 12829400]
35. Taguchi A, Blood DC, del Toro G, Canet A, Lee DC, Qu W, et al. Blockade of RAGE-amphoterin signalling suppresses tumour growth and metastases. *Nature.* 2000; 405:354–60. [PubMed: 10830965]
36. Stitt AW. The maillard reaction in eye diseases. *Ann N Y Acad Sci.* 2005; 1043:582–97. [PubMed: 16037281]
37. Reaven P, Merat S, Casanada F, Sutphin M, Palinski W. Effect of streptozotocin-induced hyperglycemia on lipid profiles, formation of advanced glycation endproducts in lesions, and extent of atherosclerosis in LDL receptor-deficient mice. *Arterioscler Thromb Vasc Biol.* 1997; 17:2250–6. [PubMed: 9351397]
38. Tezuka M, Koyama N, Morisaki N, Saito Y, Yoshida S, Araki N, et al. Angiogenic effects of advanced glycation end products of the Maillard reaction on cultured human umbilical cord vein endothelial cells. *Biochem Biophys Res Commun.* 1993; 193:674–80. [PubMed: 7685599]
39. Cross VL, Zheng Y, Won Choi N, Verbridge SS, Sutermaster BA, Bonassar LJ, et al. Dense type I collagen matrices that support cellular remodeling and microfabrication for studies of tumor angiogenesis and vasculogenesis in vitro. *Biomaterials.* 2010; 31:8596–607. [PubMed: 20727585]
40. Hermanson, GT. *Bioconjugate Techniques.* 1. Academic Press; 1996.
41. Ding Y, Kantarci A, Hasturk H, Trackman PC, Malabanan A, Van Dyke TE. Activation of RAGE induces elevated O₂- generation by mononuclear phagocytes in diabetes. *J Leukoc Biol.* 2007; 81:520–7. [PubMed: 17095613]
42. Schmidt AM, Hori O, Chen JX, Li JF, Crandall J, Zhang J, et al. Advanced glycation endproducts interacting with their endothelial receptor induce expression of vascular cell adhesion molecule-1 (VCAM-1) in cultured human endothelial cells and in mice. A potential mechanism for the accelerated vasculopathy of diabetes. *The Journal of Clinical Investigation.* 1995; 96:1395–403. [PubMed: 7544803]
43. Koka V, Wang W, Huang XR, Kim-Mitsuyama S, Truong LD, Lan HY. Advanced glycation end products activate a chymase-dependent angiotensin II-generating pathway in diabetic complications. *Circulation.* 2006; 113:1353–60. [PubMed: 16520412]
44. Mitola S, Belleri M, Urbinati C, Coltrini D, Sparatore B, Pedrazzi M, et al. Cutting Edge: Extracellular High Mobility Group Box-1 Protein Is a Proangiogenic Cytokine. *The Journal of Immunology.* 2006; 176:12–5. [PubMed: 16365390]

45. Ren X, Shao H, Wei Q, Sun Z, Liu N. Advanced Glycation End-products Enhance Calcification in Vascular Smooth Muscle Cells. *The Journal of International Medical Research*. 37:847–54. [PubMed: 19589269]
46. Quinn TM, Grodzinsky AJ. Longitudinal modulus and hydraulic permeability of poly(methacrylic acid) gels: effects of charge density and solvent content. *Macromolecules*. 1993; 26:4332–8.
47. Kraning-Rush CM, Carey SP, Califano JP, Smith BN, Reinhart-King CA. The role of the cytoskeleton in cellular force generation in 2D and 3D environments. *Phys Biol*. 2011; 8:015009. [PubMed: 21301071]
48. Carey SP, Kraning-Rush CM, Williams RM, Reinhart-King CA. Biophysical control of invasive tumor cell behavior by extracellular matrix microarchitecture. *Biomaterials*. 2012; 33:4157–65. [PubMed: 22405848]
49. Raub CB, Unruh J, Suresh V, Krasieva T, Lindmo T, Gratton E, et al. Image Correlation Spectroscopy of Multiphoton Images Correlates with Collagen Mechanical Properties. *Biophysical Journal*. 2008; 94:2361–73. [PubMed: 18065452]
50. Lutolf MP, Raeber GP, Zisch AH, Tirelli N, Hubbell JA. Cell-Responsive Synthetic Hydrogels. *Advanced Materials*. 2003; 15:888–92.
51. Raeber GP, Lutolf MP, Hubbell JA. Molecularly engineered PEG hydrogels: a novel model system for proteolytically mediated cell migration. *Biophys J*. 2005; 89:1374–88. [PubMed: 15923238]
52. Kelm JM, Timmins NE, Brown CJ, Fussenegger M, Nielsen LK. Method for generation of homogeneous multicellular tumor spheroids applicable to a wide variety of cell types. *Biotechnol Bioeng*. 2003; 83:173–80. [PubMed: 12768623]
53. Brightman AO, Rajwa BP, Sturgis JE, McCallister ME, Robinson JP, Voytik-Harbin SL. Time-lapse confocal reflection microscopy of collagen fibrillogenesis and extracellular matrix assembly in vitro. *Biopolymers*. 2000; 54:222–34. [PubMed: 10861383]
54. Williams BR, Gelman RA, Poppke DC, Piez KA. Collagen fibril formation. Optimal in vitro conditions and preliminary kinetic results. *J Biol Chem*. 1978; 253:6578–85. [PubMed: 28330]
55. Califano JP, Reinhart-King CA. Substrate stiffness and cell area drive cellular traction stresses in single cells and cells in contact. *Cellular and Molecular Bioengineering*. 2010; 3:68–75. [PubMed: 21116436]
56. Kemeny SF, Figueroa DS, Andrews AM, Barbee KA, Clyne AM. Glycated collagen alters endothelial cell actin alignment and nitric oxide release in response to fluid shear stress. *J Biomech*. 2011; 44:1927–35. [PubMed: 21555127]
57. Figueroa D, Kemeny S, Clyne A. Glycated Collagen Impairs Endothelial Cell Response to Cyclic Stretch. *Cellular and Molecular Bioengineering*. 2011; 4:220–30.
58. Provenzano PP, Inman DR, Eliceiri KW, Trier SM, Keely PJ. Contact guidance mediated three-dimensional cell migration is regulated by Rho/ROCK-dependent matrix reorganization. *Biophys J*. 2008; 95:5374–84. [PubMed: 18775961]
59. Gross J, Kirk D. The heat precipitation of collagen from neutral salt solutions: some rate-regulating factors. *J Biol Chem*. 1958; 233:355–60. [PubMed: 13563501]
60. Yang YL, Motte S, Kaufman LJ. Pore size variable type I collagen gels and their interaction with glioma cells. *Biomaterials*. 2010; 31:5678–88. [PubMed: 20430434]
61. Raub CB, Suresh V, Krasieva T, Lyubovitsky J, Mih JD, Putnam AJ, et al. Noninvasive assessment of collagen gel microstructure and mechanics using multiphoton microscopy. *Biophys J*. 2007; 92:2212–22. [PubMed: 17172303]
62. Drouven BJ, Evans CH. Collagen fibrillogenesis in the presence of lanthanides. *J Biol Chem*. 1986; 261:11792–7. [PubMed: 3745166]
63. Zhou X, Rowe RG, Hiraoka N, George JP, Wirtz D, Mosher DF, et al. Fibronectin fibrillogenesis regulates three-dimensional neovessel formation. *Genes Dev*. 2008; 22:1231–43. [PubMed: 18451110]
64. Lawrence BJ, Madhally SV. Cell colonization in degradable 3D porous matrices. *Cell Adh Migr*. 2008; 2:9–16. [PubMed: 19262124]
65. Yeung T, Georges PC, Flanagan LA, Marg B, Ortiz M, Funaki M, et al. Effects of substrate stiffness on cell morphology, cytoskeletal structure, and adhesion. *Cell Motil Cytoskeleton*. 2005; 60:24–34. [PubMed: 15573414]

66. Boobink IWG, de Boer HC, Tekelenburg WLH, Banga J-D, de Groot PG. Effect of Extracellular Matrix Glycation on Endothelial Cell Adhesion and Spreading: Involvement of Vitronectin. *Diabetes*. 1997; 46:87–93. [PubMed: 8971087]
67. McCarthy AD, Uemura T, Etcheverry SB, Cortizo AMÍa. Advanced glycation endproducts interfere with integrin-mediated osteoblastic attachment to a type-I collagen matrix. *The International Journal of Biochemistry & Cell Biology*. 2004; 36:840–8.
68. Krantz S, Lober M, Thiele M, Teuscher E. Diminished adhesion of endothelial aortic cells on fibronectin and collagen layers after nonenzymatic glycation. *Exp Clin Endocrinol*. 1988; 91:155–60. [PubMed: 3409968]
69. Bunn HF, Gabbay KH, Gallop PM. The glycosylation of hemoglobin: relevance to diabetes mellitus. *Science*. 1978; 200:21–7. [PubMed: 635569]
70. Monnier VM, Cerami A. Nonenzymatic browning in vivo: possible process for aging of long-lived proteins. *Science*. 1981; 211:491–3. [PubMed: 6779377]
71. Monnier VM, Kohn RR, Cerami A. Accelerated age-related browning of human collagen in diabetes mellitus. *Proc Natl Acad Sci U S A*. 1984; 81:583–7. [PubMed: 6582514]
72. Sims T, Rasmussen L, Oxlund H, Bailey A. The role of glycation cross-links in diabetic vascular stiffening. *Diabetologia*. 1996; 39:946–51. [PubMed: 8858217]
73. Odetti P, Rossi S, Monacelli F, Poggi A, Cirmigliaro M, Federici M, et al. Advanced glycation end products and bone loss during aging. *Ann N Y Acad Sci*. 2005; 1043:710–7. [PubMed: 16037297]
74. Kaji Y, Usui T, Oshika T, Matsubara M, Yamashita H, Araie M, et al. Advanced glycation end products in diabetic corneas. *Invest Ophthalmol Vis Sci*. 2000; 41:362–8. [PubMed: 10670463]
75. Verzijl N, DeGroot J, Thorpe SR, Bank RA, Shaw JN, Lyons TJ, et al. Effect of collagen turnover on the accumulation of advanced glycation end products. *J Biol Chem*. 2000; 275:39027–31. [PubMed: 10976109]
76. Vitek MP, Bhattacharya K, Glendening JM, Stopa E, Vlassara H, Bucala R, et al. Advanced glycation end products contribute to amyloidosis in Alzheimer disease. *Proc Natl Acad Sci U S A*. 1994; 91:4766–70. [PubMed: 8197133]
77. Takahashi M, Kushida K, Ohishi T, Kawana K, Hoshino H, Uchiyama A, et al. Quantitative analysis of crosslinks pyridinoline and pentosidine in articular cartilage of patients with bone and joint disorders. *Arthritis Rheum*. 1994; 37:724–8. [PubMed: 8185700]
78. Donnelly SM. Accumulation of glycated albumin in end-stage renal failure: evidence for the principle of “physiological microalbuminuria”. *Am J Kidney Dis*. 1996; 28:62–6. [PubMed: 8712223]
79. Lopez JI, Kang I, You W-K, McDonald DM, Weaver VM. In situ force mapping of mammary gland transformation. *Integrative Biology*. 2011; 3:910–21. [PubMed: 21842067]
80. DITZEL JR. Angioscopic Changes in the Smaller Blood Vessels in Diabetes Mellitus and their Relationship to Aging. *Circulation*. 1956; 14:386–97. [PubMed: 13365051]
81. Carmeliet P, Jain RK. Angiogenesis in cancer and other diseases. *Nature*. 2000; 407:249–57. [PubMed: 11001068]

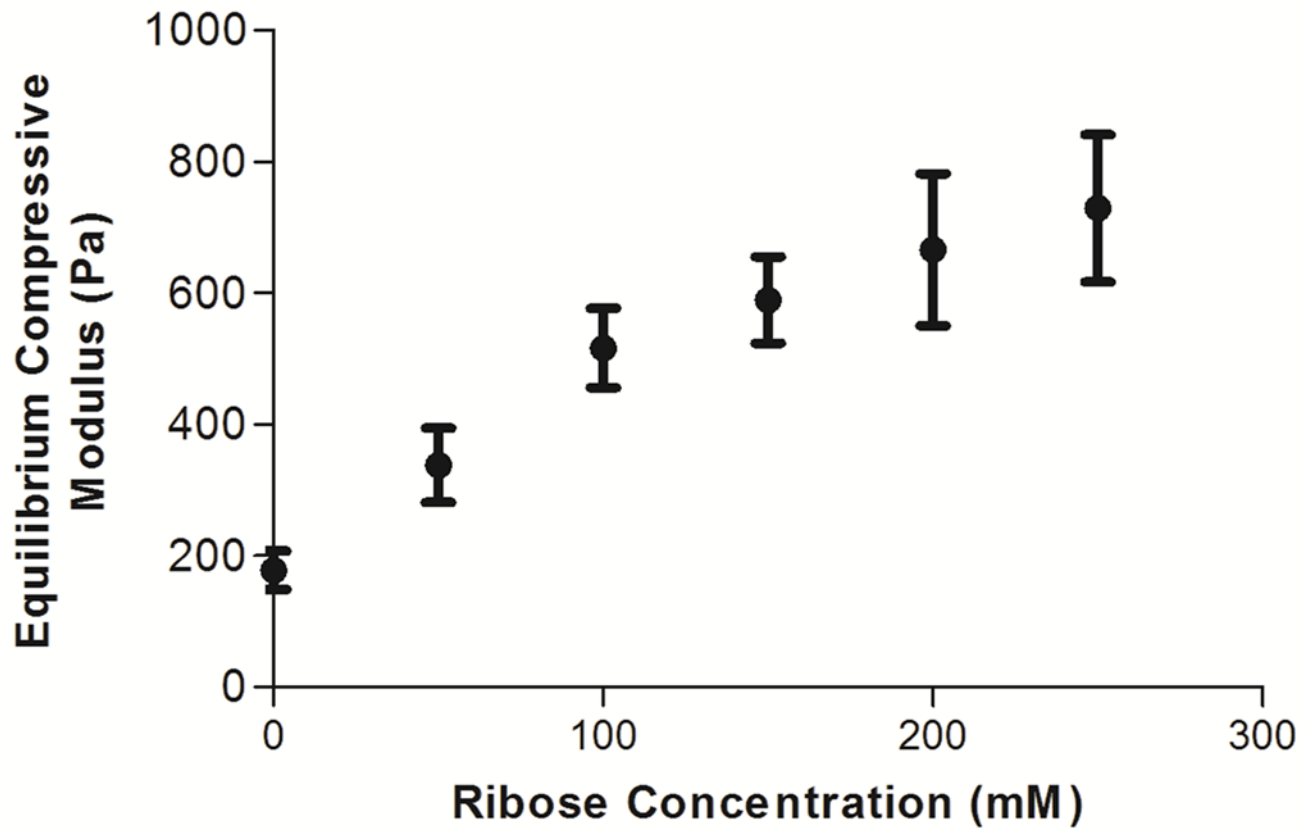


Figure 1. Collagen gel mechanical properties. The equilibrium compressive moduli of 1.5 mg/mL collagen gels were measured by confined compression testing. Data presented as mean \pm SEM

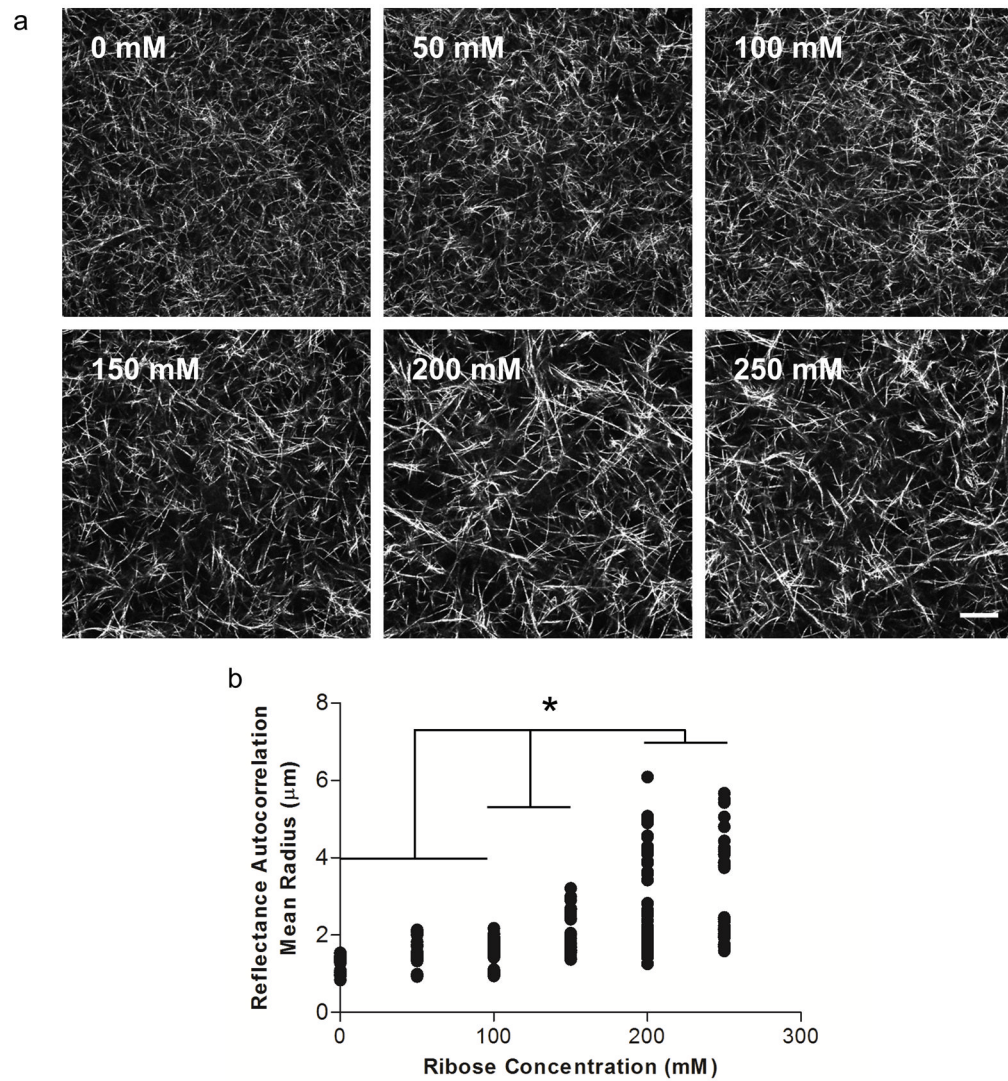


Figure 2. The effects of non-enzymatic glycation on collagen fibril arrangement and organization. (a) Confocal reflectance microscopy was used to image the collagen gels formed from solutions that had been incubated with 0, 50, 100, 150, 200, or 250 mM ribose. (b) Collagen fiber organizations were compared using the image autocorrelation mean radius. Scale is 20 μm

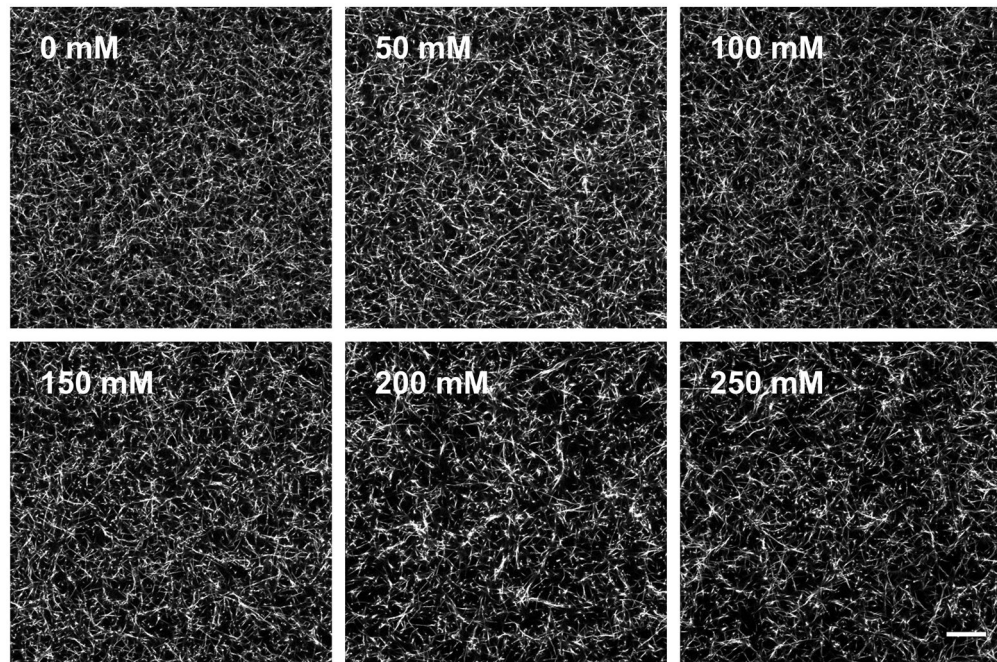


Figure 3. The effects of non-enzymatic glycation on fluorescently-labeled collagen fibril arrangement. TRITC-labeled collagen was incubated with 0, 50, 100, 150, 200, or 250 mM ribose and imaged with fluorescence microscopy. Scale is 20 μm

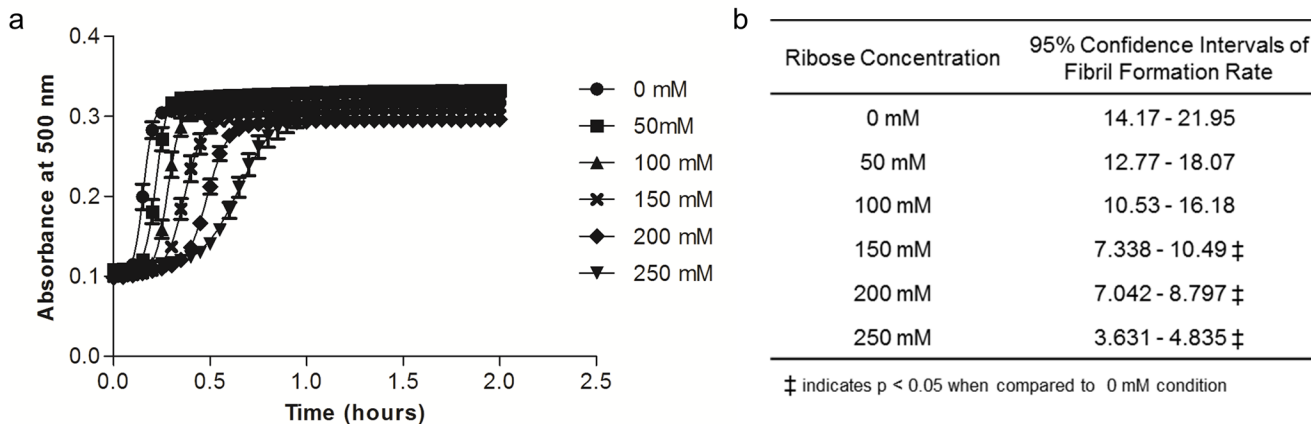


Figure 4.

The effects of non-enzymatic glycation on the polymerization dynamics of collagen. (a) Collagen polymerization dynamics were measured as a function of ribose concentration based on absorbance readings at 500 nm during polymerization. (b) The fibril formation rates of glycated collagen polymerization were found by fitting a sigmoidal curve to the polymerization data in (a) and reporting the slope of the linear section of the curve. Data presented as mean \pm SEM

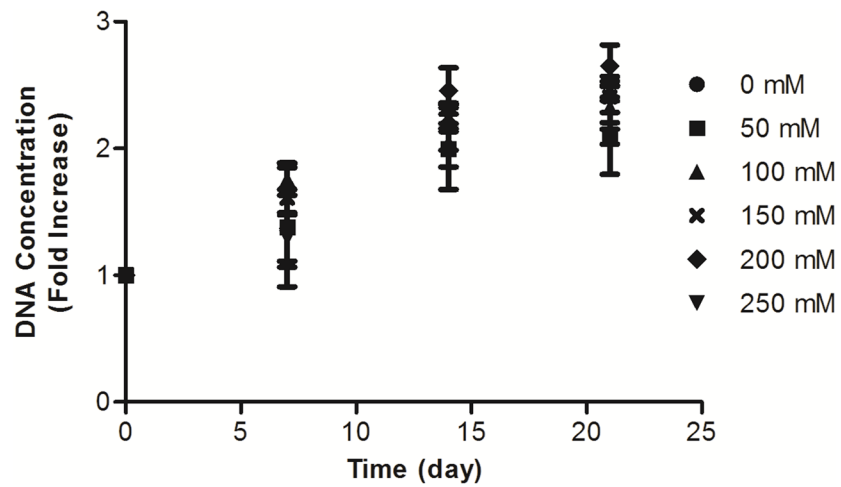


Figure 5. Endothelial cell proliferation within glycosylated collagen gels. ECs were embedded within collagen gels that had been glycosylated with 0, 50, 100, 150, 200, or 250 mM ribose. Cellular viability and proliferation was assessed by measuring the DNA content of gels at 0, 7, 14, or 21 days.

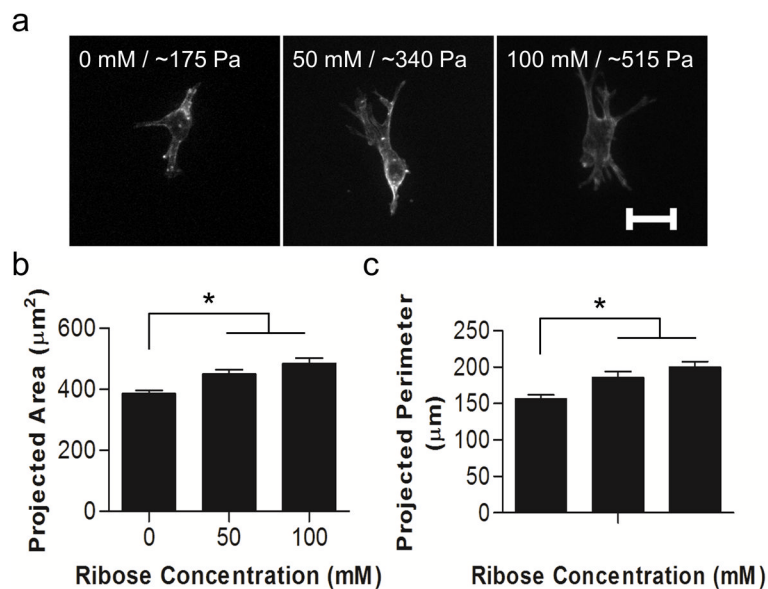


Figure 6. Single cell response to matrix stiffness. Isolated ECs were embedded within collagen gels formed from solutions that had been incubated with 0, 50, or 100 mM ribose. Cells were allowed to spread for 24 hours and then were fixed and stained for actin. (a) ECs were imaged using confocal microscopy and the projected cell (a) area and (b) perimeter were determined. Data presented as mean + SEM, * indicates $p < 0.05$, Scale is 20 μm

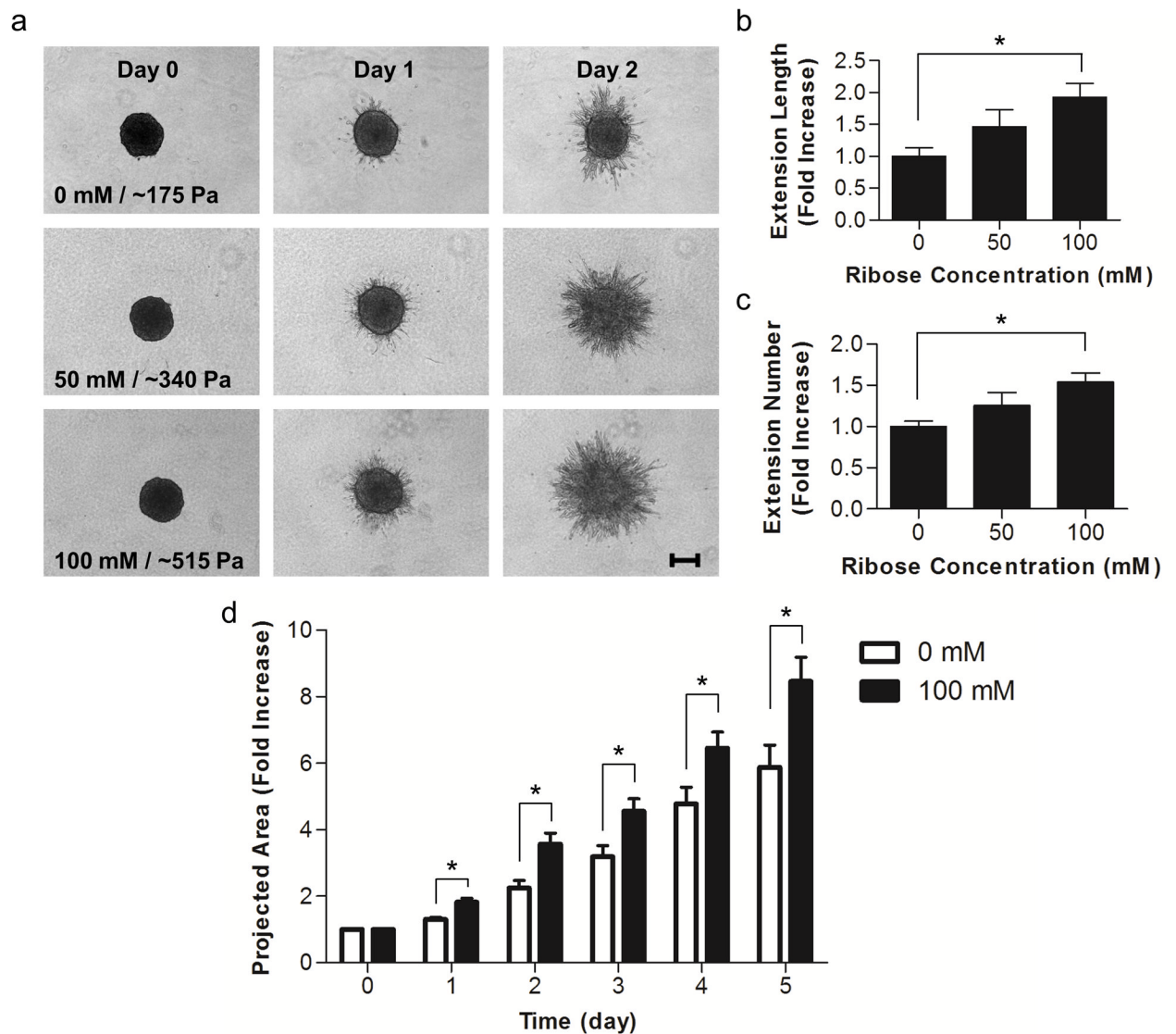


Figure 7.

Angiogenic outgrowth response to matrix stiffness. Multi-cellular spheroids were embedded within collagen polymerized from solutions treated with 0, 50, or 100 mM ribose. (a) Spheroids were imaged using brightfield microscopy at 0, 1, and 2 days after embedding. (b) The total length of extensions and (c) the average number of extensions per spheroid were measured at day 1. (d) The projected spheroid area, including the extensions, was measured over the course of 5 days. Data presented as mean + SEM, * indicates $p < 0.05$, Scale is 200 μm

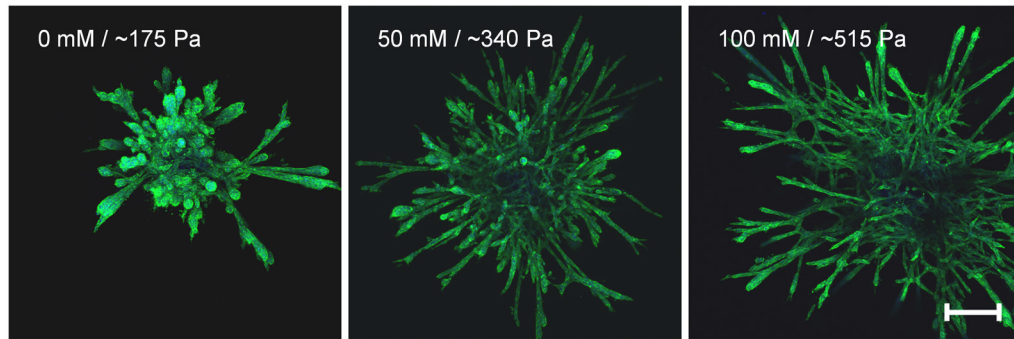


Figure 8.

Long-term angiogenic outgrowth response to matrix stiffness. Multi-cellular spheroids were grown in collagen gels polymerized from solutions treated with 0, 50, or 100 mM ribose for 8 days. Spheroids were fixed and stained for actin and DAPI and imaged using confocal microscopy. Scale is 200 μm

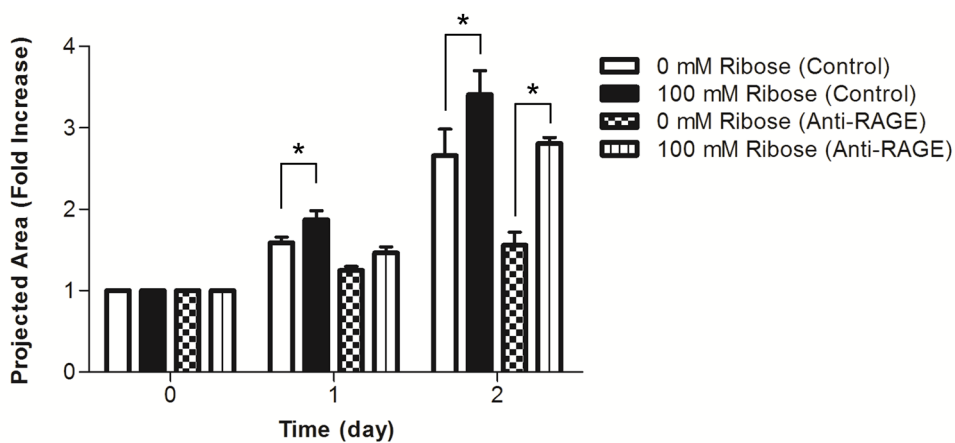


Figure 9.

The effects of RAGE inhibition on spheroid outgrowth. Multi-cellular spheroids were embedded within collagen polymerized from solutions treated with 0 or 100 mM ribose and fed at 1 hour with either complete media with or without 10 μ g/ml anti-RAGE blocking antibody. (a) The projected spheroid areas were measured at days 0, 1, and 2 after embedding. Data presented as mean + SEM, * indicates $p < 0.05$